Frontiers of Information Technology & Electronic Engineering
www.zju.edu.cn/jzus; engineering.cae.cn; www.springerlink.com
ISSN 2095-9184 (print); ISSN 2095-9230 (online)
E-mail: jzus@zju.edu.cn

A novel period estimation method for X-ray pulsars based on frequency subdivision*

Li-rong SHEN‡, Xiao-ping LI, Hai-feng SUN, Hai-yan FANG, Meng-fan XUE

(*School of Aerospace Science and Technology, Xidian University, Xi'an 710071, China*)

E-mail: slr_xidian@163.com; xpli@xidian.edu.cn; sunhaifeng@163.com;
hyfang@xidian.edu.cn; xuemf@163.com

Received Feb. 9, 2015; Revision accepted June 19, 2015; Crosschecked Sept. 9, 2015

Abstract: Period estimation of X-ray pulsars plays an important role in X-ray pulsar based navigation (XPNAV). The fast Lomb periodogram is suitable for period estimation of X-ray pulsars, but its performance in terms of frequency resolution is limited by data length and observation time. Longer observation time or oversampling can be employed to improve frequency analysis results, but with greatly increased computational complexity and large amounts of sampling data. This greatly restricts real-time autonomous navigation based on X-ray pulsars. To resolve this issue, a new method based on frequency subdivision and the continuous Lomb periodogram (CLP) is proposed to improve precision of period estimation using short-time observation data. In the proposed method, an initial frequency is first calculated using fast Lomb periodogram. Then frequency subdivision is performed near the initial frequency to obtain frequencies with higher precision. Finally, a refined period is achieved by calculating the CLP in the obtained frequencies. Real data experiments show that when observation time is shorter than 135 s, the proposed method improves period estimation precision by 1–3 orders of magnitude compared with the fast Lomb periodogram and fast Fourier transform (FFT) methods, with only a slight increase in computational complexity. Furthermore, the proposed method performs better than efsearch (a period estimation method of HEAsoft) with lower computational complexity. The proposed method is suitable for estimating periods of X-ray pulsars and obtaining the rotation period of variable stars and other celestial bodies.

Key words: Pulsar navigation, Period estimation, Frequency subdivision, Continuous Lomb periodogram
doi:10.1631/FITEE.1500052 **Document code:** A **CLC number:** V448; P128.4

1 Introduction

Pulsars are rapidly rotating neutron stars emitting stable and regular signals (Manchester and Taylor, 1977; Lyne and Graham-Smith, 2006). They have been observed in radio, visible, X-ray, and gamma-ray bands of the electromagnetic spectrum (Sheikh, 2005; Shuai, 2009). These pulsars have been considered to be a novel approach for assisting deep space navigation. X-ray signals can be detected by a small and light X-ray detector placed on the spacecraft, which can help reduce the power consumption and mass of the spacecraft. In addition, X-ray pulsars have good spatial distribution in the sky, which enhances their observability (Emadzadeh and Speyer, 2011). As a new feasible navigation method for deep space exploration, X-ray pulsar based navigation (XPNAV) was firstly proposed by Chester and Butman (1981). In recent years, XPNAV has been investigated by many researchers (Hanson, 1996; Emadzadeh and Speyer, 2011; Xiong *et al.*, 2012; Feng *et al.*, 2013; Liu *et al.*, 2014; Wang *et al.*, 2014; Zhang *et al.*, 2014).

The basic observation of XPNAV is the time-of-arrival (TOA) of X-ray photons (Sheikh, 2005).

‡ Corresponding author
* Project supported by the National Basic Research Program (973) of China (No. 2014CB340205), the National Natural Science Foundation of China (Nos. 61301173 and 61473228), and the Aerospaced TT&C Innovation Program of 704 Research Institute of China (No. 201405B)
ORCID: Li-rong SHEN, http://orcid.org/0000-0002-9131-1079

Comparing the integrated pulse profile at the spacecraft with the standard pulse profile at the solar system barycenter (SSB), a pulse TOA can be obtained (Liu *et al.*, 2012). Since an X-ray pulsar signal is extremely weak when it reaches a spacecraft, folding the pulse profile and estimating the TOA, pulsar period with high precision is important (Xie, 2012). As is well known, some pulsars have good long-term stabilities similar to today's atomic clocks (Kaspi *et al.*, 1994; Matsakis *et al.*, 1997; Lyne and Graham-Smith, 2006), but the stabilities are not good in short-time span. Moreover, the Doppler effect generated by movement of spacecraft may lead to changes of the observed signal frequency. If a short-term period or frequency is not estimated, folding X-ray photon TOAs using a fixed period will result in a deformed profile (Xie, 2012; Sun *et al*., 2013). Consequently, positioning precision will be reduced as well.

The main goal of this paper is to provide a feasible, effective, and high-precision period estimation method for X-ray pulsars using the data observed in a short-time span. This method facilitates the real-time period estimation and updating, which will greatly improve the precision of TOA estimation as well as position and velocity measurements in XPNAV.

The Fourier transform method (Xie, 2012) is often applied to periodic signal studies and has low computational complexity. However, in a situation where there is a low signal-to-noise ratio (SNR), power 'leakage' can easily mask any steep variation in the spectrum. Moreover, this method is limited in dealing with unevenly sampled data (Scott *et al.*, 2003; Zhang *et al.*, 2012), which is common in astronomical observations, unless the data is interpolated to assume that the observations are adequate. The chi-square method (Stellingwerf, 1978; Leahy *et al.*, 1983; Mao, 2009) estimates a period by calculating chi-square values of observation data in different candidate periods. Using this method, the correct period refers to a maximum chi-square value. However, the precision of this method depends on the initial period value and search range, which have not been determined with any clarity. Consequently, the method becomes highly complex if there is a situation of high precision period estimation. An effective method was proposed for period estimation of pulsars (Li and Ke, 2010; Li *et al.*, 2012). Using this method, coherent statistics of a cyclostationary signal are adopted. Compared with the classical Fourier transform method, this method performs better when SNR is low, with a cost of increasing computational complexity. Zhou *et al.* (2013) presented a period estimation method for X-ray pulsars. The initial period value is calculated using a fast Lomb periodogram, and then the period is refined by the chi-square method. This method realizes high precision period estimation using simulation data, but does not work with real data. Although the methods mentioned above are able to estimate period values for pulsars, they are not able to fulfil the requirement for high precision measurements, especially in the case of short-term observation with low SNR. To the best of our knowledge, frequency estimation precision of existing models is generally below 10^{-5} Hz, and period estimation precision is generally below 10^{-8} s in a short-time span of observation (Li and Ke, 2010; Li *et al.*, 2012; Zhou *et al.*, 2013).

Since X-ray photons which arrive at the detector are unevenly spaced, a method of processing unevenly spaced data is needed for period estimation.

Fast Lomb periodogram (Lomb, 1976; Scargle, 1982; Press and Rybicki, 1989; Schulz and Stattegger, 1997; Laguna *et al.*, 1998; Zhou *et al.*, 2013; Jenkins *et al.*, 2014) is a classical method for processing unevenly spaced time series. Similar to power spectrum analysis, fast Lomb periodogram has been widely applied in the processing of astronomical data. Therefore, it is suitable for processing X-ray pulsar signals. However, its use has been limited to data sets, the size of which is generally no longer than 10^6 on a computer (Press and Rybicki, 1989). Meanwhile, the precision of this method is limited by observation time and data length. Reducing the 'picket fence effect' and 'spectrum leakage' (Hu, 2003) is vital in this method. To alleviate the problems, oversampling (Zhou *et al.*, 2013) is often exploited. Regrettably, oversampling will lead to a great amount of sampling data, which will inevitably increase the computational burden. In addition, the observation time of the X-ray pulsar should not be too long, meaning that only limited data can be received in real-time spacecraft navigation. Consequently, false peaks occurring in the Lomb periodogram may lead to an incorrect pulsar periodization.

To improve the precision of period estimation for X-ray pulsars using the data observed in a short-time

span, in this paper, we propose a new local frequency subdivision based method. This method is able to significantly improve precision of period estimation for X-ray pulsars only at the cost of a slight increase in computational complexity. Experimental results show that the proposed method achieves a high period estimation precision of 10^{-9} s when the observation time is 132 s. In deep space exploration, the pulsar period with high precision will facilitate better positioning precision for spacecraft in XPNAV.

2 Period estimation method based on discrete Fourier transform

The discrete Fourier transform (DFT) is a commonly used method with low computational complexity in processing periodic signals. Since TOAs of X-ray photons are unevenly spaced, the DFT method cannot be directly used.

To take advantage of the DFT method to analyze X-ray pulsar signals, a common approach is to transform the TOAs of X-ray photons into equally spaced TOAs using interpolation.

Let t_i be the TOA of the ith photon. The number of the TOAs of the photons in t_i is $y_N(t_i)=y_i$, and $y_N(t_i)$ is an energy-limited signal, where N is the length of the time series. First, smoothing and interpolation are employed to turn unevenly spaced time series into evenly spaced time series, obtaining $\hat{y}(t_i)=\hat{y}_i$. Second, conduct spectrum analysis by using DFT:

$$Y(k)=\sum_{n=0}^{\hat{N}-1}\hat{y}_i\exp\left(-\mathrm{j}\frac{2\pi}{\hat{N}}nk\right),\ k=0,1,...,\hat{N}-1, \quad (1)$$

where $\hat{N}$ is the length of time series after interpolation.

Third, one must square the amplitude $Y(k)$ and divide it by $\hat{N}$ (Hu, 2003), which produces

$$P_{\mathrm{PER}}(k)=\frac{1}{\hat{N}}|Y(k)|^2. \quad (2)$$

The results of $P_{\mathrm{PER}}(k)$ can reflect the estimation of real power spectrum $P(\mathrm{e}^{\mathrm{j}\omega})$.

Finally, the best frequency corresponding to the significant peak of P_{PER} will determine the pulsar period, which can be computed as

$$T=1/f_{\mathrm{opt}}=1\Big/\arg\max_{f\in[f_{\min},f_{\max}]}P_{\mathrm{PER}}, \quad (3)$$

where $[f_{\min}, f_{\max}]$ is the known and finite span containing the exact frequency f_{opt} ($f_{\mathrm{opt}}=1/T$).

Although DFT can be implemented by fast Fourier transform (FFT) with low computational complexity, it is not robust if a situation of low SNR arises. Power 'leakage' may easily mask any steep variation in the spectrum. Consequently, a false period is obtained. Even though smoothing and interpolation can alleviate the problems of 'spectrum leakage' and 'picket fence effect', sometimes smoothing may cause signal information loss, while interpolation may cause a frequency shift (Zhou *et al.*, 2013). In addition, another characteristic of DFT is that it is not able to effectively reflect the spectrum characteristics of unevenly spaced data because it is based on evenly spaced data. Thus, DFT is not sufficient to accurately estimate the period for an X-ray pulsar.

3 New period estimation method based on frequency subdivision

In this section, we first briefly outline the advantages and disadvantages of fast Lomb periodogram. Then based on this method, a new period estimation method which can make the period estimation of an X-ray pulsar more accurate, is demonstrated in detail.

3.1 Fast Lomb periodogram

Consider a set of N observations y_i at times t_i (i=1, 2, …, N) with the mean of $\bar{y}$ and a variance of σ^2. Set up the signal model as follows:

$$y_i=a\cos(\omega t_i)+b\sin(\omega t_i)+n_i, \quad (4)$$

where noises n_i are independent with zero mean and a variance of σ_n^2, a and b are unknown parameters, and ω is the given angular frequency. The least squares method is generally used to calculate coefficients.

The Lomb normalized periodogram which is the spectral power as a function of ω (Lomb, 1976; Scargle, 1982), is constructed as follows:

$$P_N(\omega)=\frac{1}{2\sigma^2}\left\{\frac{\left[\sum_i(y_i-\overline{y})\cos(\omega(t_i-\tau))\right]^2}{\sum_i\cos^2(\omega(t_i-\tau))}+\frac{\left[\sum_i(y_i-\overline{y})\sin(\omega(t_i-\tau))\right]^2}{\sum_i\sin^2(\omega(t_i-\tau))}\right\}, \tag{5}$$

where τ is a constant time offset which makes $P_N(\omega)$ completely independent of all the t_i's constant shifting. The relationship between τ and t_i is as follows:

$$\tan(2\omega\tau)=\frac{\sum_i\sin(2\omega t_i)}{\sum_i\cos(2\omega t_i)}. \tag{6}$$

The frequency corresponding to the significant peak of Lomb periodogram determines the X-ray pulsar period:

$$T=2\pi/\omega=2\pi/\arg\max P_N(\omega). \tag{7}$$

Technically, Lomb periodogram requires a number of operations approximating $10^2N_\omega N$ to examine N_ω frequencies for a data set of N points (Press and Rybicki, 1989), which implies that this method has high computational complexity. Subsequently, the calculation efficiency of Lomb periodogram can be improved by adopting the calculating method of FFT, which makes the operation count approximating only $N_\omega\log N_\omega$ (Press and Rybicki, 1989). The details of the calculation are listed in the Appendix.

As the sampling theorem is suitable only for evenly spaced data, the precise Nyquist frequency cannot be obtained in the analysis of the TOAs of X-ray photons using fast Lomb periodogram. To solve this problem, an average Nyquist frequency (Schulz and Stattegger, 1997), $f_{\mathrm{Nyq}}=1/(2\Delta t)$ with Δt being the average sampling span, is employed in this paper. Therefore, frequency resolution of fast Lomb periodogram can be obtained as follows:

$$\Delta f=f_{\mathrm{s}}/N=1/(N\cdot\Delta t)\approx 1/T_{\mathrm{obs}}, \tag{8}$$

where T_{obs} is the total observation time and f_{s} the sampling frequency.

Obviously, the frequency resolution is inversely proportional to the observation time and data length. The longer the observation time, the larger the number of photons, and the higher the frequency resolution. As a result, a higher period estimation precision can be ensured.

The inverse of the time span of the input data determines the lowest independent frequency of fast Lomb periodogram:

$$f_{\min}=1/(t_{\max}-t_{\min})=1/T_{\mathrm{obs}}, \tag{9}$$

where $t_{\min}$ is the arrival time of the first photon and $t_{\max}$ the arrival time of the last photon.

The highest independent frequency $f_{\max}$ can be determined as follows:

$$f_{\max}=N/T_{\mathrm{obs}}. \tag{10}$$

This fast Lomb method reduces both computational burden and running time of Lomb periodogram, but the precision of this method is also limited by data length and observation time. To properly collect and evaluate data peaks which have statistical significance, longer observation time or oversampling is employed, which leads to a considerable increase in data volume, operation time, and computational complexity.

3.2 Proposed novel period estimation method

To improve the precision of period estimation for X-ray pulsars using the data observed in a short-time span, a continuous Lomb periodogram (CLP) based on local frequency subdivision is proposed below.

Assuming that the frequency f is a continuous variable in a specified frequency range $[f_1, f_2]$, the frequency resolution will not be limited by the observation time.

Based on the definition of DFT (Scargle, 1982) for unevenly spaced data, we define a DFT for X-ray pulsar signals as follows:

$$X(f)=\sqrt{N_0}\sum_{i=1}^{N_0}y_i\left[A\cos(2\pi ft_i)+\mathrm{j}B\sin(2\pi ft_i)\right], \tag{11}$$

where N_0 is the total number of independent frequencies, and A and B are unspecified functions of f which may depend on t_i. The corresponding periodogram is

$$\begin{aligned}P(f)&=(1/N_0)\cdot|X(f)|^2\\&=\left[A\sum_i y_i\cos(2\pi ft_i)\right]^2+\left[B\sum_i y_i\sin(2\pi ft_i)\right]^2.\end{aligned} \tag{12}$$

To obtain a similar analysis to the fast Lomb method, we choose

$$A(f)=\left[\sum_i \cos^2(2\pi f t_i)\right]^{-1/2}, \tag{13}$$

$$B(f)=\left[\sum_i \sin^2(2\pi f t_i)\right]^{-1/2}. \tag{14}$$

Substituting Eqs. (13) and (14) into Eq. (12), we obtain

$$P(f)=\frac{1}{\sigma^2}\left\{\frac{\left[\sum_i (y_i-\bar{y})\cos(2\pi f(t_i-\tau))\right]^2}{\sum_i \cos^2(2\pi f(t_i-\tau))}+\frac{\left[\sum_i (y_i-\bar{y})\sin(2\pi f(t_i-\tau))\right]^2}{\sum_i \sin^2(2\pi f(t_i-\tau))}\right\}. \tag{15}$$

To make $P(f)$ completely independent of all the t_i's shifting by any constant for each frequency f of interest, compute a time-offset τ by

$$\tau(f)=\frac{1}{2\times 2\pi f}\arctan\left[\frac{\sum_i \sin(2\times 2\pi f t_i)}{\sum_i \cos(2\times 2\pi f t_i)}\right]. \tag{16}$$

The time-offset τ affects only phase but not amplitude. If X-ray pulsar photons arriving at the detector are evenly spaced, τ=0.

Recall the set of N observations y_i at times t_i (i=1, 2, …, N). The total observation time T_{obs} includes at least one period of the X-ray pulsar. First, the initial frequency f_{first} can be estimated using an effective method. Second, the first frequency subdivision based on the frequency initial value at a short frequency interval $[f_1, f_2]$ is conducted to obtain frequencies f_j (j=1, 2, …, $\hat{n}$) with higher precision satisfying $f_1<f_{\text{first}}<f_2$. Third, one must calculate $P(f_j)$ which corresponds to frequency values f_j. Then frequency f_{1_best} with higher precision corresponding to the peak of $P(f_j)$ can be obtained. Finally, based on f_{1_best}, subsequent frequency subdivision can be conducted in a shorter frequency interval $[f_{1i}, f_{2i}]$ to obtain frequencies f_{ij} with a higher frequency resolution, where i (i=1, 2, …, M) is the number of times that frequency subdivision occurs, satisfying $f_{1i}<f_{i\_\text{best}}<f_{2i}$ and $f_1<f_{1i}<f_{2i}<f_2$.

Therefore, the best frequency corresponding to the significant peak of the CLP $P_i(f_j)$ will determine the higher precision period for the X-ray pulsar:

$$T=1/f_{i\_\text{best}}=1\Big/\arg\max_{f_j\in[f_{1i},f_{2i}]} P_i(f_j). \tag{17}$$

3.3 Definitions of the higher precision frequency resolution and frequencies

To reduce computational complexity, we subdivide the frequency layer by layer, and each subdivision contains j frequencies. Then $P(f_j)$ which corresponds to higher precision frequency values is calculated.

The number of times that frequency subdivision must occur depends on the value of precision. The frequency resolution with higher precision is determined by

$$\Delta f=m^{-(i+1)}, \tag{18}$$

where m and i are positive integers. Generally, for i=1, the value of m is 10, 100, or 1000, and the frequency resolution will be 0.01, 0.001, or 0.0001 Hz, respectively. If $i\geq 2$, frequency resolution will be higher. In this paper, we set m=10.

To obtain frequencies with higher precision and avoid subdivision with extreme ranges which influence the accuracy of frequency estimation, we specify the initial frequency and more accurate frequencies based on experience precision of fast Lomb periodogram, as described below:

1. The initial frequency f_{first} is calculated by using fast Lomb periodogram.

2. To obtain the precise value of $m^{-(i+1)}$ of f_{i_best}, we overlap the subdivided frequency value. In each frequency subdivision, the value of m^{-i} of f_{i_best} is retained, ignoring the values of $m^{-(i+1)}$ of f_{i_best}, for $i\geq 1$.

Subsequently, frequency subdivision values are calculated using

$$f_{\text{mid}\_i}(j)=\begin{cases}\text{floor}(f_{\text{first}})+j\cdot\Delta f, & i=1,\\ \dfrac{\text{floor}(f_{i\_\text{best}}\cdot m^{i-1})}{m^{i-1}}+j\cdot\Delta f, & i\geq 2,\end{cases} \tag{19}$$

where floor(x) denotes the largest integer no more than x, i is the number of times that frequency is

subdivided, j (j=1, 2, …, $\hat{n}$) is the number of frequencies, and f_{i_best}, with respect to the peak of $P_i(f_j)$, is the best frequency of the ith frequency subdivision and the corresponding calculation of CLP. The value of $\hat{n}$ depends on the frequency resolution. To reduce computational complexity without sacrificing the accuracy, we set $\hat{n}=m^2$.

After i rounds of subdivision, the estimation precision of frequency will reach $m^{-(i+1)}$ Hz, which will assure a fairly accurate period value.

We then analyze the computational complexity of the CLP method, which is approximately $\hat{n}\cdot N$, where $\hat{n}$ is the number of subdivision frequencies, and $\hat{n}\ll N$. Although the computational complexity of the CLP method is higher than that of fast Lomb periodogram and FFT (both about $N\log N$), it is lower than that of the chi-square method (about N^2).

4 Real data experiments and discussion

In this section, the proposed method is demonstrated using the real data of the Crab pulsar observed by the Rossi X-ray Timing Explorer (RXTE) satellite. We will first outline and preprocess the RXTE data. Then we conduct period estimation for the X-ray pulsar using the short-term observation data.

4.1 Observation data and preprocessing

On Dec. 30, 1995, the RXTE satellite was launched into low-Earth orbit to observe black holes, neutron stars, X-ray pulsars, and bursts of X-rays, and was decommissioned on Jan. 5, 2012. Much of the astronomical data collected has been made public.

RXTE data is the Flexible Image Transport System (FITS) format maintained by the High Energy Astrophysics Science Archive Research Center (HEASARC) (ftp://legacy.gsfc.nasa.gov/xte/nra/appendix_f/RXTE_tech_append.pdf).

The proportional counter array (PCA) is the main detector of the RXTE satellite with 1 μs time resolution. The proportional counters of PCA cover the 2–60 keV range and are effective over an area of about 6500 cm^2. Thus, a large number of the X-ray pulsar photon series are collected by PCA. Science array and science event are basic formats of PCA data (Ge, 2012). The science array format is used for data binned at regular intervals, and the science event format is used for unbinned data. The data of two formats is recorded based on the terrestrial time system.

The Crab pulsar is a young pulsar with better known ephemeris and high-flux X-ray emissions. It is also a candidate for XPNAV. In addition, a larger amount of Crab pulsar observation data is available. Therefore, in this paper we choose PCA science event format data to estimate the Crab pulsar period.

However, serious interferences originating from the cosmic background radiation and other sources have contaminated X-ray photons from the Crab pulsar. Therefore, to estimate a correct period for the Crab pulsar, observation data preprocessing is necessary. In addition, to compute accurate arrival times of pulses in XPNAV, measurements must be made relative to an inertial frame, generally the SSB, which is an unaccelerated frame with respect to pulsars. Therefore, to conduct time transformation, some sources of time delay should be taken into consideration, including the Roemer, Einstein, and Shapiro delay. In this paper, HEAsoft is adopted to preprocess the X-ray photons. The details are outlined as follows:

Step 1: Identify the files which contain the data needed using the GUI-driven program ‘XDF’ (XTE data finder).

Step 2: Produce filter files using ‘xtefilt’ to identify and screen good data.

Step 3: Obtain the good time span using ‘maketime’.

Step 4: Conduct barycenter corrections and obtain the corrected photon TOAs using ‘fasebin’.

Note that ‘XDF’, ‘xtefilt’, ‘maketime’, and ‘fasebin’ are the tools of HEAsoft.

Before showing the difference between the raw and preprocessed photon TOAs, it is important to briefly outline ‘efsearch’. Subsequently, the period estimation can be conducted using the raw and preprocessed photon TOAs to verify the importance of data preprocessing in period estimation.

‘Efsearch’ (https://heasarc.gsfc.nasa.gov/ftools/ftools_menu.html) is a special tool of HEAsoft used for X-ray pulsar period estimation. It searches for periodicities in a time series by folding the data over a range of periods and by searching for a maximum chi-square as a function of period. As efsearch is limited to processing FITS format data, the preprocessed photon TOAs are saved in text format. To be

able to estimate period using the preprocessed photon TOAs, efsearch is implemented by MATLAB and its input format is extended without changing the algorithm or results. This means that efsearch can be used more conveniently. Period estimation results from the Crab pulsar using the raw data packet 90802-02-04-00 are shown in Figs. 1 and 2.

From Figs. 1 and 2 we can see that the chi-square values obtained by the extended efsearch are the same as those of efsearch. So, in the following sections, efsearch and the extended efsearch are collectively referred to as efsearch. To verify the effectiveness of the CLP method, the performance of CLP will be compared with that of efsearch.

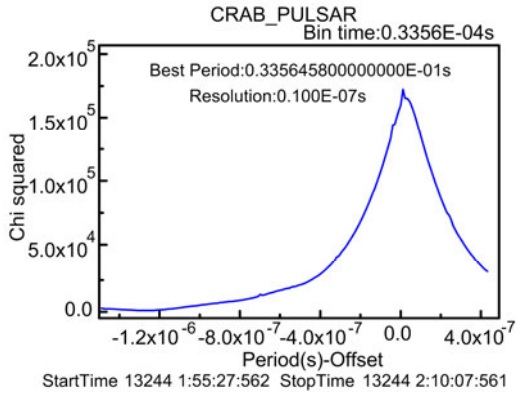

Fig. 1 Period estimation using efsearch in HEAsoft

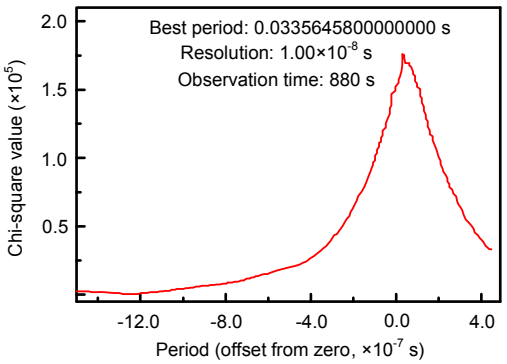

Fig. 2 Period estimation using the extended efsearch in MATLAB (Crab pulsar, bin time: 3.356×10^{-5} s)

Finally, data packet 90802-02-04-00 from the Crab pulsar is selected and preprocessed following the steps outlined above. Then efsearch is used to estimate the period for the Crab pulsar using both the raw and preprocessed photon TOAs. The analysis results are shown in Table 1.

As indicated in Table 1, the difference between the raw and preprocessed photon TOAs is large. Due to data preprocessing, invalid photon TOAs have been filtered out and several delays have been corrected. Therefore, the number of photon TOAs after preprocessing has decreased and the effective observation time is less than the total observation time. After analysis, the difference between the estimated frequencies when using the raw and preprocessed photon TOAs being attributed to the Doppler effect is confirmed.

If the period is estimated using the raw photon TOAs, the estimated period will gravely deviate from the true period. Consequently, significant errors will occur in TOA estimation and XPNAV.

Table 1 Difference between the raw and preprocessed photon TOAs

Item	Raw	Preprocessed
NUM	9 091 449	7 653 921
T_{obs} (s)	880	738.9009
P_{est} (s)	0.033 564 594 7	0.033 566 924 4
F_{est} (Hz)	29.793 298 75	29.791 230 99

NUM: number of the photons; T_{obs}: observation time; P_{est}: estimated period; F_{est}: estimated frequency

4.2 Performance of the proposed method

In this paper, the running time and absolute value of the mean error between the real and estimated pulsar periods are used to assess the performance of the proposed method.

The period estimation mean error (PEME) is defined as follows:

$$\mathrm{PEME}(s)=\frac{1}{N}\sum_{i=1}^{N}|s_c-s_e|, \tag{20}$$

where s_c stands for the real pulsar period or the real pulsar frequency, s_e stands for the estimated pulsar period or the estimated pulsar frequency, and N is the number of times that period estimation is undertaken.

To realize the real-time navigation based on X-ray pulsar, in this paper, we estimate mainly the period for the Crab pulsar using the preprocessed photon TOAs received in a short observation time.

First, we select 1 379 832 photon TOAs in an observation time of 132 s from data packet 90802-

02-04-00. Then the CLP method, fast Lomb method, FFT method, and efsearch are used to estimate the period under the same conditions. Finally, we compare the period estimation precision of the CLP method with that of other three methods.

In this paper, the sampling interval of the FFT method is 0.01 μs. The frequency resolution of fast Lomb is determined by the total observation time, with an oversampling rate of 4. Efsearch is conducted in three steps and the initial period is 0.0335 s with the search range of (0.0335, 0.0336) s. In each step, the resolution is 1, 0.1, and 0.01 μs respectively, and 2000 candidate periods are analyzed. At the same time, the same amount of data is used to calculate the initial frequency and conduct frequency subdivision in the CLP method, which performs seven times frequency subdivision with the frequency resolution of $10^{-(i+1)}$ Hz, for i=1, 2, …, 7, and 100 frequencies are obtained in each subdivision. These frequencies will be used for the calculation of CLP to obtain the best frequency. The PEMEs of the four methods are shown in Table 2.

Table 2 PEME of the Crab pulsar using four methods

Method	PEME(f) (Hz)	PEME(p) (s)
Fast Lomb	4.02×10^{-4}	4.53×10^{-7}
FFT	1.29×10^{-3}	1.45×10^{-6}
Efsearch	6.70×10^{-5}	7.54×10^{-8}
CLP	2.15×10^{-6}	2.42×10^{-9}

Table 2 shows that the period estimation precision of the CLP method is 2 orders of magnitude higher than that of the fast Lomb method, 3 orders of magnitude higher than that of the FFT method, and 1 order of magnitude higher than that of efsearch. Even if a situation arises whereby the flux of the nebulae background is about 9 times more than the X-ray pulsar signals, we can see that the period estimation precision of the CLP method can reach 2.42×10^{-9} s, and the frequency estimation precision can reach 2.15×10^{-6} Hz, which is very useful in realizing XPNAV.

Generally, to reach a velocity estimation precision of hundreds of meters per second using the Doppler effect, the frequency estimation precision needs to reach 10^{-6} Hz. From the analysis above, we can see that in deep space exploration, the CLP method can help reach a velocity estimation precision of hundreds of meters per second using the data observed during 132 s in XPNAV.

To demonstrate the significant influence of the period on pulse profile folding, integrated pulse profiles are firstly folded by using different periods which are being estimated using four methods. Then the integrated pulse profiles are compared with the standard pulse profile. The results are shown in Fig. 3.

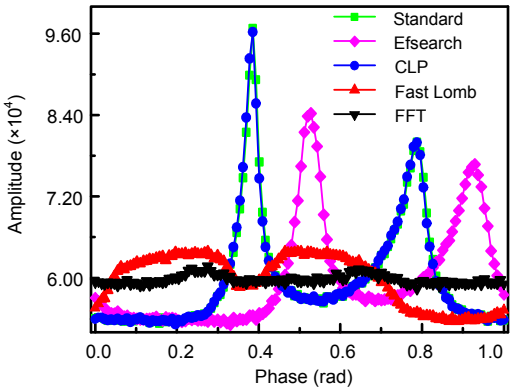

Fig. 3 Comparison between the standard profile and integrated pulse profiles

Fig. 3 indicates that using the CLP method can help obtain a clear pulse profile which matches the standard pulse profile well. Likewise, efsearch can help generate a pulse profile. However, the pulse profile is deformed by a phase delay compared with the standard pulse profile. The fast Lomb method and FFT method are not able to achieve a clear pulse profile due to the low period estimation precision.

As the amount of data varies in different data packets, and the data of different packets is observed at different intervals, the period estimation results are different to the others. To further assess the validity of the proposed CLP method, the other two data packets, 90802-02-02-00 and 90802-02-06-00, are tested. After data preprocessing, the period is estimated using the preprocessed photon TOAs, which are observed in different time spans. The period estimation results are shown in Figs. 4 and 5.

From Figs. 4 and 5 we can see that the period estimation results of the two data packets are slightly different. However, the period estimation mean errors of all the four methods decrease gradually with the growth of the observation time. It is therefore possible to assert that the proposed CLP method performs better than the other three methods.

To further analyze the period estimation mean errors of the CLP method and the other three methods, 10 data packets are further tested from 90802-02-02-00 to 90802-02-17-00, and any glitch is removed from the data. First, each data packet is divided into several subintervals according to the observation time. Then the pulsar period is estimated using the data of each subinterval. Finally, the PEMEs of the estimated period results are calculated (Table 3).

Table 3 indicates that the PEMEs of the four methods decrease gradually with the growth of the observation time, and that the CLP method has the minimal PEME in a short-time span. These results further verify the effectiveness of the proposed CLP method.

The precision of the four methods is related to the data length. The longer the observation time, the greater the data length, and the higher the period estimation precision.

The efsearch method demonstrates high precision period estimation over a long observation time with a large amount of observation data (Fig. 6). However, in the short observation time span, the observation data is limited with low SNR. It is easy to generate some burrs in calculated chi-square values (Fig. 7). The burrs are sometimes considered to be the maximum of chi-square values. Consequently, it will lead to significant period estimation errors.

Fig. 8 shows the integrated pulse profiles folded using the correct period corresponding to the maximum of chi-square values and the incorrect period corresponding to the burrs in the chi-square values.

As shown in Fig. 8, the difference between the integrated profiles is very large. The correct period can help obtain a clear pulse profile, while the incorrect period cannot, which indicates that efsearch does not perform well over a short observation time.

As is well known, the frequency resolutions of the fast Lomb method and the FFT method are

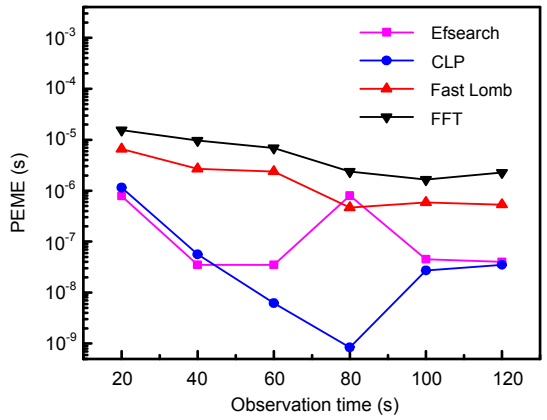

Fig. 4 PEME of the four methods using the data of packet 90802-02-02-00

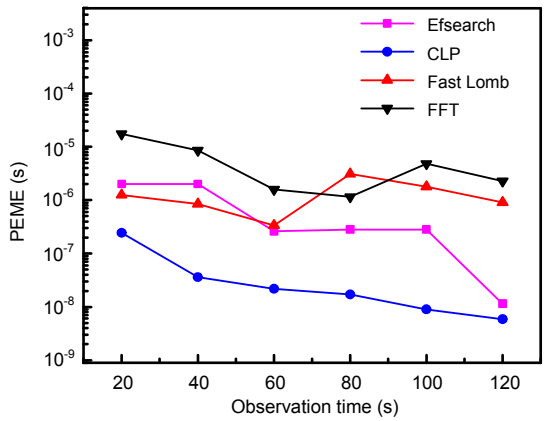

Fig. 5 PEME of the four methods using the data of packet 90802-02-06-00

Table 3 PEME(p) of the four methods

Observation time (s)	PEME(p) (s)			
	FFT	Fast Lomb	Efsearch	CLP
20	1.54×10^{-5}	1.45×10^{-5}	7.72×10^{-6}	8.88×10^{-7}
40	6.66×10^{-6}	6.71×10^{-6}	3.58×10^{-6}	2.91×10^{-7}
60	4.49×10^{-6}	4.53×10^{-6}	9.07×10^{-7}	1.33×10^{-7}
80	4.01×10^{-6}	3.98×10^{-6}	7.28×10^{-7}	1.29×10^{-7}
100	2.88×10^{-6}	2.85×10^{-6}	1.28×10^{-7}	5.36×10^{-8}
120	1.94×10^{-6}	1.93×10^{-6}	6.38×10^{-8}	4.40×10^{-8}

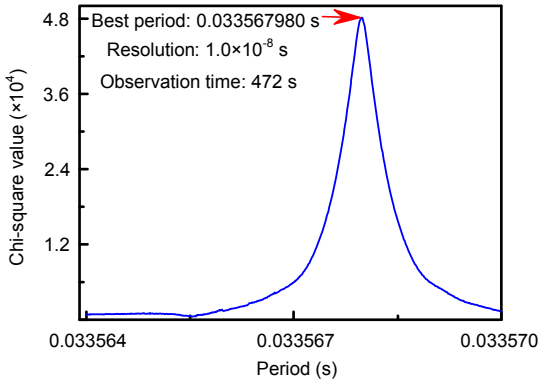

Fig. 6 High precision period estimated using the long-time observation data of packet 90802-02-06-00 (Crab pulsar, bin time: 3.356×10^{-5} s)

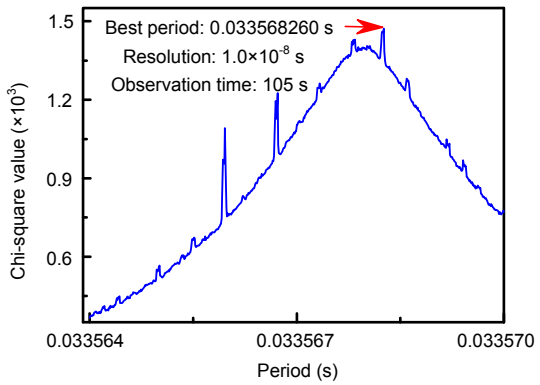

Fig. 7 Low precision period estimated using the short-time observation data of packet 90802-02-06-00 (Crab pulsar, bin time: 3.356×10^{-5} s)

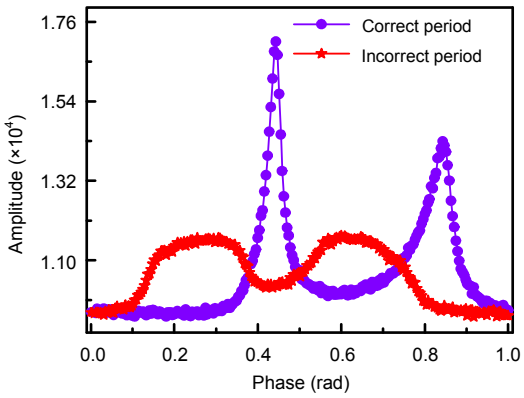

Fig. 8 Integrated profiles folded using correct and incorrect periods

inversely proportional to the observation time. If the observation time is known, the data length will be fixed. As a result, the frequency resolution will be determined. Oversampling or using a small sample of intervals is sometimes employed to try and resolve problems such as the 'picket fence effect' and the 'spectrum leakage' as well as to help identify possible peaks in the spectrum. However, the frequency resolution has not changed because the total observation time is still T.

Thus, due to limited data length and low SNR, the fast Lomb method and FFT are not able to estimate a correct period for pulsars using the data observed in a short time. This is particularly relevant for the FFT method, as it is suitable for the evenly spaced data, while the TOAs of X-ray photons are not. Thus, its performance is not reliable.

The proposed CLP method is able to detect and analyze any peak occurring in the CLP, which benefits from frequency subdivision. In each frequency subdivision, the period is estimated only in a smaller range determined by the best frequency obtained by the last calculation of the CLP. This strategy is used to avoid the interference from noises which exist in a large range. In addition, it is worth mentioning that the CLP is a special periodogram analysis method for unevenly spaced data. Therefore, the CLP method is very appropriate when estimating the period for an X-ray pulsar.

In addition, in this paper the mean running time of the four methods can be used to reflect the performance of the four methods (Fig. 9).

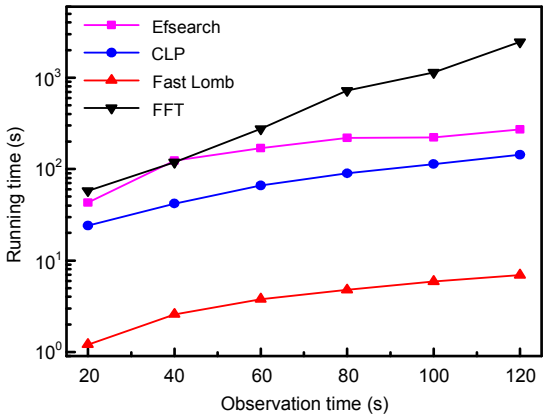

Fig. 9 Mean running time of the four methods

To keep the conditions the same as in the other three methods, the sample interval is set as 0.01 μs for FFT, which leads to the highest computational complexity among the four methods.

Efsearch has the second largest running time, because it is a blind search method. This method needs a large running time to search for a better initial period value and then perform further estimation. Due to the imprecise period estimation which results from using only one step, in this paper period estimation using efsearch is conducted in three steps. Obviously, this method is time-consuming when the initial period and the search range are unknown.

The CLP method analyzes the spectrum in limited frequencies, which are obtained by frequency subdivision. At the same time, this method can avoid the larger amount of sampling data produced by oversampling or the use of a much smaller sample interval. Therefore, the advantages listed above and

the effective calculation of the initial frequency can reduce the running time of the CLP method compared with that of efsearch, while it is still longer than that of the fast Lomb method.

The running time of the fast Lomb periodogram is the shortest among the four methods. This can be explained by the fact that the calculating method of FFT is adopted, which makes the running time of this method noticeably decrease.

The analysis above demonstrates the advantages of the CLP method and its utility in realizing a high precision period estimation for X-ray pulsars using short-term observation data. Thus, the CLP method is effective in helping realize real-time period updating, in obtaining more accurate time delay estimation, and in improving the precision of real-time positioning and velocity measurement based on X-ray pulsars navigation.

5 Conclusions

To improve the precision of period estimation for X-ray pulsars using the data observed in a short-time span, a new method based on frequency subdivision and CLP is proposed. Using this method, the initial frequency is first calculated using fast Lomb periodogram. Then frequency subdivision is performed near the initial frequency. Finally, a refined period, which has higher precision, is achieved by calculating CLP from the obtained frequencies. The real data of the Crab pulsar observed by the RXTE satellite has been used to verify the effectiveness of the CLP method. The results of the experiment show that the period estimation precision of the CLP method is 1–3 orders of magnitude higher than that of the fast Lomb method and FFT method, and that the CLP method is more effective than efsearch when using the same amount of data.

The proposed method also indicates that the observed data within 120–130 s can be used to estimate and update the period for XPNAV. This period will significantly improve the precision of the folding profile and time delay estimation as well as position and velocity measurement in deep space exploration based on X-ray pulsar navigation. The method is also applicable when seeking to measure the rotation period of other variable stars and celestial bodies.

Acknowledgements

The authors would like to thank Drs. Wen-ying LEI and Wen-bo ZHAO from Xidian University, Hong-dou LIU from Northwest University, and Guang SUN from Aerors Inc. for refining this paper.

References

Chester, T.J., Butman, S.A., 1981. Navigation Using X-Ray Pulsers. TDA Progress Report 42-63, p.22-25.

Emadzadeh, A.A., Speyer, J.L., 2011. Relative navigation between two spacecraft using X-ray pulsars. *IEEE Trans. Contr. Syst. Technol.*, **19**(5):1021-1035. [doi:10.1109/TCST.2010.2068049]

Feng, D.J., Xu, L.P., Zhang, H., *et al*., 2013. Determination of inter-satellite relative position using X-ray pulsars. *J. Zhejiang Univ.-Sci. C (Comput. & Electron.)*, **14**(2):133-142. [doi:10.1631/jzus.C12a0142]

Ge, M.Y., 2012. The X-Ray Emission of Pulsar. PhD Thesis, University of Chinese Academy of Sciences, China (in Chinese).

Hanson, J.E., 1996. Principles of X-Ray Navigation. SLAC-Report-809, Stanford University, USA.

Hu, G.S., 2003. Digital Signal Processing: Theory, Methods and Implementation. Tsinghua University Press, China (in Chinese).

Jenkins, J.S., Yoma, N.B., Rojo, P., *et al*., 2014. Improved signal detection algorithms for unevenly sampled data. Six signals in the radial velocity data for GJ876. *Mon. Not. R. Astron. Soc*., **441**(3):2253-2265. [doi:10.1093/mnras/stu683]

Kaspi, V.M., Taylor, J.H., Ryba, M.F., 1994. High-precision timing of millisecond pulsars. III: long-term monitoring of PSRs B1855+09 and B1937+21. *Astrophys. J.*, **428**(2):713-728.

Laguna, P., Moody, G.B., Mark, R.G., 1998. Power spectral density of unevenly sampled data by least-square analysis: performance and application to heart rate signals. *IEEE Trans. Biomed. Eng.*, **45**(6):698-715. [doi:10.1109/10.678605]

Leahy, D.A., Darbro, W., Elsner, R.F., *et al*., 1983. On searches for pulsed emission with application to four globular cluster X-ray sources: NGC 1851, 6441, 6624, and 6712. *Astrophys. J.*, **266**:160-170.

Li, J.X., Ke, X.Z., 2010. Period estimation method for weak pulsars based on coherent statistic of cyclostationary signal. *Acta Phys. Sin.*, **59**(11):8304-8310 (in Chinese).

Li, J.X., Ke, X.Z., Zhao, B.S., 2012. A new time-domain estimation method for period of pulsars. *Acta Phys. Sin.*, **61**(6):069701.1-069701.7 (in Chinese).

Liu, J., Ma, J., Tian, J.W., *et al*., 2012. Pulsar navigation for interplanetary missions using CV model and ASUKF. *Aerosp. Sci. Technol.*, **22**(1):19-23. [doi:10.1016/j.ast.2011.04.010]

Liu, J., Fang, J.C., Ning, X.L., *et al*., 2014. Closed-loop EKF-based pulsar navigation for Mars explorer with

Doppler effects. *J. Navig.*, **67**(5):776-790. [doi:10.1017/S0373463314000216]

Lomb, N.R., 1976. Least-squares frequency analysis of unequally spaced data. *Astrophys. Space Sci.*, **39**(2):447-462. [doi:10.1007/BF00648343]

Lyne, A.G., Graham-Smith, F., 2006. Pulsar Astronomy. Cambridge University Press, UK.

Manchester, R.N., Taylor, J.H., 1977. Pulsars. W. H. Freeman, San Francisco, USA.

Mao, Y., 2009. Research on X-Ray Pulsar Navigation Algorithms. PhD Thesis, The PLA Information Engineering University, Zhengzhou, China (in Chinese).

Matsakis, D.N., Taylor, J.H., Eubanks, T.M., 1997. A statistic for describing pulsar and clock stabilities. *Astron. Astrophys.*, **326**:924-928.

Press, W.H., Rybicki, G.B., 1989. Fast algorithm for spectral analysis of unevenly sampled data. *Astrophys. J.*, **338**:227-280.

Scargle, J.D., 1982. Studies in astronomical time series analysis. II: statistical aspects of spectral analysis of unevenly spaced data. *Astrophys. J.*, **263**:835-853.

Schulz, M., Stattegger, K., 1997. Spectrum: spectral analysis of unevenly spaced paleoclimatic time series. *Comput. Geosci.*, **23**(9):929-945. [doi:10.1016/s0098-3004(97)00087-3]

Scott, D.M., Finger, M.H., Wilson, C.A., 2003. Characterization of the timing noise of the Crab pulsar. *Mon. Not. R. Astron. Soc.*, **344**(2):412-430. [doi:10.1046/j.1365-8711.2003.06825.x]

Sheikh, S.I., 2005. The Use of Variable Celestial X-Ray Sources for Spacecraft Navigation. PhD Thesis, University of Maryland, USA.

Shuai, P., 2009. Principle and Method of the X-Ray Pulsar Navigation System. China Aerospace Press, China (in Chinese).

Stellingwerf, R.F., 1978. Period determination using phase dispersion minimization. *Astrophys. J.*, **224**:953-960.

Sun, H.F., Xie, K., Li, X.P., *et al*., 2013. A simulation technique of X-ray pulsar signals with high timing stability. *Acta Phys. Sin.*, **62**(10):109701.1-109701.11 (in Chinese). [doi:10.7498/aps.62.109701]

Wang, Y.D., Zheng, W., Sun, S.M., *et al*., 2014. X-ray pulsar-based navigation using time-differenced measurement. *Aeros. Sci. Technol.*, **36**:27-35. [doi:10.1016/j.ast.2014.03.007]

Xie, Q., 2012. Study on Signal Identification and Cycle Ambiguity Resolution Technology for X-Ray Pulsar. PhD Thesis, Xidian University, China (in Chinese).

Xiong, Z., Qiao, L., Liu, J.Y., *et al*., 2012. Geo satellite autonomous navigation using X-ray pulsar navigation and GNSS measurements. *Int. J. Innov. Comput. Inform. Contr.*, **8**(5A):2965-2977.

Zhang, C.H., Wang, N., Yuan, J.P., *et al.*, 2012. Timing noise study of four pulsars. *Sci. China Phys. Mech. Astron.*, **55**(2):333-338. [doi:10.1007/s11433-011-4620-6]

Zhang, H., Xu, L.P., Shen, Y.H., *et al*., 2014. A new maximum-likelihood phase estimation method for X-ray pulsar signals. *J. Zhejiang Univ.-Sci. C (Comput. & Electron.)*, **15**(6):458-469. [doi:10.1631/jzus.C1300347]

Zhou, Q.Y., Ji, J.F., Ren, H.F., 2013. Quick search algorithm of X-ray pulsar period based on unevenly spaced timing data. *Acta Phys. Sin.*, **62**(1):019701.1-019701.8 (in Chinese).

Appendix: Fast Lomb periodogram evaluation

To approximately calculate Eqs. (5) and (6) (Press and Rybicki, 1989), we define the following four simpler sums:

$$\begin{cases} S_{\mathrm{h}} = \sum_{j=1}^{N} (y_j - \overline{y}) \sin(\omega t_j), \\ C_{\mathrm{h}} = \sum_{j=1}^{N} (y_j - \overline{y}) \cos(\omega t_j), \end{cases} \tag{A1}$$

$$\begin{cases} S_2 = \sum_{j=1}^{N} \sin(2\omega t_j), \\ C_2 = \sum_{j=1}^{N} \cos(2\omega t_j). \end{cases} \tag{A2}$$

Then we can obtain

$$\begin{aligned} &\sum_{j=1}^{N} (y_j - \overline{y}) \sin(\omega(t_j - \tau)) \\ &= \sum_{j=1}^{N} (y_j - \overline{y}) \sin(\omega t_j) \cos(\omega\tau) \\ &\quad - \sum_{j=1}^{N} (y_j - \overline{y}) \cos(\omega t_j) \sin(\omega\tau) \\ &= S_{\mathrm{h}} \cos(\omega\tau) - C_{\mathrm{h}} \sin(\omega\tau), \end{aligned} \tag{A3}$$

and

$$\begin{aligned} &\sum_{j=1}^{N} (y_j - \overline{y}) \cos(\omega(t_j - \tau)) \\ &= \sum_{j=1}^{N} (y_j - \overline{y}) \cos(\omega t_j) \cos(\omega\tau) \\ &\quad - \sum_{j=1}^{N} (y_j - \overline{y}) \sin(\omega t_j) \sin(\omega\tau) \\ &= C_{\mathrm{h}} \cos(\omega\tau) + S_{\mathrm{h}} \sin(\omega\tau). \end{aligned} \tag{A4}$$

Subsequently, the following formulas can be obtained:

$$\begin{aligned}\sum_{j=1}^{N}\sin^2(\omega(t_j-\tau)) &= \sum_{j=1}^{N}\frac{1-\cos(2\omega(t_j-\tau))}{2}\\ &= \frac{N}{2}-\frac{1}{2}\sum_{j=1}^{N}\cos(2\omega t_j)\cos(2\omega\tau)\\ &\quad -\frac{1}{2}\sum_{j=1}^{N}\sin(2\omega t_j)\sin(2\omega\tau)\\ &= \frac{N}{2}-\frac{1}{2}C_2\cos(2\omega\tau)-\frac{1}{2}S_2\sin(2\omega\tau),\end{aligned} \tag{A5}$$

$$\begin{aligned}\sum_{j=1}^{N}\cos^2(\omega(t_j-\tau)) &= \sum_{j=1}^{N}\frac{1+\cos(2\omega(t_j-\tau))}{2}\\ &= \frac{N}{2}+\frac{1}{2}\sum_{j=1}^{N}\cos(2\omega t_j)\cos(2\omega\tau)\\ &\quad +\frac{1}{2}\sum_{j=1}^{N}\sin(2\omega t_j)\sin(2\omega\tau)\\ &= \frac{N}{2}+\frac{1}{2}C_2\cos(2\omega\tau)+\frac{1}{2}S_2\sin(2\omega\tau),\end{aligned} \tag{A6}$$

where t_j in above formulas must be evenly spaced. However, the photon TOAs are unevenly spaced. To obtain the evenly spaced t_j, reverse interpolation can be employed to turn unevenly spaced time series into evenly spaced time series.

Finally, the four quantities S_h, C_h, S_2, and C_2 can be evaluated by two complex FFTs, and the results can be substituted back through Eqs. (A3)–(A6) to evaluate the following equation:

$$\begin{aligned}P_N(\omega) &= \frac{1}{2\sigma^2}\left\{\frac{\left[\sum_i (y_i-\bar{y})\cos(\omega(t_i-\tau))\right]^2}{\sum_i \cos^2(\omega(t_i-\tau))}\right.\\ &\quad \left.+\frac{\left[\sum_i (y_i-\bar{y})\sin(\omega(t_i-\tau))\right]^2}{\sum_i \sin^2(\omega(t_i-\tau))}\right\}\\ &= \frac{1}{2\sigma^2}\left\{\frac{[C_h\cos(\omega\tau)+S_h\sin(\omega\tau)]^2}{N/2+1/2\cdot C_2\cos(2\omega\tau)+1/2\cdot S_2\sin(2\omega\tau)}\right.\\ &\quad \left.+\frac{[S_h\cos(\omega\tau)-C_h\sin(\omega\tau)]^2}{N/2-1/2\cdot C_2\cos(2\omega\tau)-1/2\cdot S_2\sin(2\omega\tau)}\right\}.\end{aligned} \tag{A7}$$